Phase mixing of relativistically intense waves in a cold homogeneous plasma

Sudip Sengupta,* Vikrant Saxena, Predhiman K. Kaw, Abhijit Sen, and Amita Das
Institute for Plasma Research, Bhat, Gandhinagar 382 428, India

(Received 27 May 2008; revised manuscript received 13 December 2008; published 20 February 2009)

We report on spatiotemporal evolution of relativistically intense longitudinal electron plasma waves in a cold homogeneous plasma, using the physically appealing Dawson sheet model. Calculations presented here in the weakly relativistic limit clearly show that under very general initial conditions, a relativistic wave will always phase mix and eventually break at arbitrarily low amplitudes, in a time scale $\omega_{pe}\tau_{mix} \sim \{\frac{3}{64}(\omega_{pe}^2\delta^3/c^2k^2)[|\Delta k/k|/(|1+\Delta k/k|)](1+1/|1+\Delta k/k|)\}^{-1}$. We have verified this scaling with respect to amplitude of perturbation δ and width of the spectrum $(\Delta k/k)$ using numerical simulations. This result may be of relevance to ultrashort, ultraintense laser pulse-plasma interaction experiments where relativistically intense waves are excited.

DOI: 10.1103/PhysRevE.79.026404 PACS number(s): 52.35.Mw, 52.27.Ny, 52.65.Rr

I. INTRODUCTION

The study of spatiotemporal evolution of relativistically intense large amplitude $(eE/m\omega_p c \sim 1)$ nonlinear plasma waves in a cold homogeneous plasma is a subject of fundamental interest to nonlinear plasma theory. Practically, nonlinear plasma waves having relativistically large amplitudes arise in a number of situations involving interaction of an ultrashort, ultraintense ($\geqslant 10^{18}$ W/cm^2, for a 1 μm wavelength laser) laser pulse or an electron beam pulse (0.5 GeV, carrying 1 kA current, focussed to 3 μm spot size $\approx 10^{18}$ W/cm^2) with a plasma. Experiments on laser assisted nuclear fusion and particle acceleration (laser-plasma wakefield acceleration) are examples of this kind. In laser fusion experiments, an intense laser pulse falls on an overdense plasma and excites plasma waves through mode conversion whereas in particle acceleration experiments, an intense laser pulse or electron beam propagating through an underdense plasma excites a large amplitude wakefield which then traps background plasma electrons or externally injected electrons and accelerates them to high energies. Amplitudes of these relativistically intense waves are limited by wave breaking which happens through a variety of nonlinear effects. Physically, plasma waves break when neighboring electron orbits cross, thus leading to conversion of coherent wave motion into random particle motion. In laser fusion experiments, wave breaking results in generation of energetic electrons which eventually leads to heating of the core and in particle accelerator experiments, wave breaking limits the maximum achievable "useful" accelerating electric field. Thus in both these situations, a pertinent issue regarding large amplitude plasma waves is the maximum magnitude of the wave electric field that can be attained without wave breaking.

It is now common knowledge that in a cold homogeneous plasma with infinitely massive ions, coherent wave motion can occur provided the Akhiezer-Polovin limit is satisfied, i.e., $eE/m\omega_{pe}c < \sqrt{2}[\gamma_{ph}-1]^{1/2}$ [1] (where $\gamma_{ph}=[1-v_{ph}^2/c^2]^{-1/2}$). Modification to this expression due to thermal motion of electrons have also been evaluated [2–5]. Regarding this cold plasma relativistic wave breaking limit, a point needs to be emphasized here is that, this wave breaking limit has been derived for a wave (or a nonlinear structure) moving with a constant phase velocity v_{ph}. This can either be a single wave with well defined ω and k or a very special combination of (ω,k) and its harmonics such that they propagate together as a coherent nonlinear mode (e.g., cold plasma Bernstein-Greene-Kruskal (BGK) modes [6] in the case of nonrelativistic waves). In a realistic ultrashort ultrahigh intensity laser-plasma interaction experiment, it is likely that a spectrum of plasma waves with an arbitrary spread in Δk (and hence in Δv_{ph}) is excited due to group velocity dispersion and nonlinear distortion of the light pulse near the critical layer [7–10]. In this regard, it becomes imperative to ask whether the Akhiezer-Polovin wave breaking limit really holds for arbitrary initial conditions?

In this paper, we address this question by studying the evolution of two relativistically intense waves having wave numbers separated by an amount Δk, both analytically and numerically. Using the physically appealing Dawson sheet model [11] we show that under very general initial conditions, a relativistic wave will always break at arbitrarily low amplitudes via a phenomenon called phase mixing; and hence the observation of wave breaking phenomenon is not limited in general by the Akhiezer-Polovin criterion.

In Sec. II, we present the relativistic equation of motion of an electron sheet and its solution using the Bogoliubov and Krylov method of averaging. Section II A contains the solution for a particular set of initial conditions representing two waves having wave numbers separated by an amount Δk. This solution clearly exhibits the phenomenon of phase mixing. In Sec. II B, we analytically demonstrate that phase mixing eventually leads to the appearance of density spikes (wave breaking). Here we also make an estimate of the time scale $(\omega_{pe}\tau_{mix})$ in which a relativistically intense wave will break via the process of phase mixing, and it dependence on the amplitude "δ" and the width of the spectrum "$\Delta k/k$." In Sec. III, using a code based on Dawson sheet model, we numerically demonstrate the phenomenon of phase mixing and the gradual progress towards wave breaking. We also numerically verify the scaling of $\omega_{pe}\tau_{mix}$ on δ and $\Delta k/k$. Finally Sec. IV contains our conclusion.

*sudip@ipr.res.in

II. EQUATION OF MOTION AND APPROXIMATE SOLUTION

We start with the relativistic equation of motion of a sheet which is given as

$$\frac{d}{d\tau}\frac{\dot{\xi}}{\sqrt{1-\frac{\dot{\xi}^2}{c^2}}} = -\frac{e}{m}E(x,t), \tag{1}$$

where $x=x_0+\xi(x_0,\tau)$, ξ being the displacement of the sheet from its equilibrium position x_0 (Lagrange coordinate), x is its Euler coordinate and the dot represents differentiation with respect to Lagrange time τ. The momentum of the sheet is given by $p=m\gamma v=m\dot{\xi}/\sqrt{1-\dot{\xi}^2/c^2}$ and electric field on the sheet is given by Gauss' law as $E=4\pi n_0 e\xi$, n_0 being the equilibrium number density. Using this expression for electric field in Eq. (1), the equation of motion becomes

$$\frac{\ddot{\xi}}{\left(1-\frac{\dot{\xi}^2}{c^2}\right)^{3/2}} + \omega_{\mathrm{pe}}^2\xi = 0, \tag{2}$$

where $\omega_{\mathrm{pe}}^2=4\pi n_0 e^2/m$ is the nonrelativistic plasma frequency. In the weakly relativistic limit, Eq. (2) reduces to

$$\ddot{\xi} + \omega_{\mathrm{pe}}^2\xi - \frac{3}{2}\frac{\omega_{\mathrm{pe}}^2}{c^2}\xi\dot{\xi}^2 \approx 0. \tag{3}$$

Using the Bogoliubov and Krylov method of averaging [12] the solution of Eq. (3) can be written as

$$\xi(x_0,\tau) \approx \xi_0(x_0)\sin[\tilde{\omega}_{\mathrm{pe}}\tau + \phi_0(x_0)], \tag{4}$$

where

$$\tilde{\omega}_{\mathrm{pe}} \approx \omega_{\mathrm{pe}}\left(1-\frac{3}{16}\frac{\omega_{\mathrm{pe}}^2\xi_0^2(x_0)}{c^2}\right). \tag{5}$$

The second term in Eq. (5) gives the nonlinear frequency shift due to relativistic variation of electron mass. The solution given by Eq. (4) and the nonlinear frequency shift [Eq. (5)] depend upon two unknown functions of x_0 *viz.* $\xi_0(x_0)$ and $\phi_0(x_0)$. These are determined from the initial conditions of the problem. In the subsection below, we determine them for a set of initial conditions representing two waves having wave numbers separated by an amount Δk.

A. Phase mixing

We choose the initial electron density and velocity profile, respectively, as

$$n_e(x,0) = n_0\left[1+\delta\cos\left(\frac{\Delta k}{2}x\right)\cos\left(k+\frac{\Delta k}{2}\right)x\right] \tag{6}$$

and

$$v_e(x,0) = \frac{\omega_{\mathrm{pe}}\delta}{2}\left[\frac{1}{k}\cos(kx)+\frac{1}{k+\Delta k}\cos(k+\Delta k)x\right]. \tag{7}$$

In the linear nonrelativistic limit these represent the initial conditions for two propagating sinusoidal waves with amplitude δ whose wave numbers differ by an amount Δk. $\Delta k \to 0$ and $\Delta k=-2k$, respectively, represent the initial condition for a single wave with well defined ω and k and a standing wave (oscillation). Using the above two initial conditions we now determine the two unknown functions $\xi_0(x_0)$ and $\phi_0(x_0)$ as follows. Using the initial velocity profile (7), we get

$$\xi_0(x_0)\cos[\phi_0(x_0)] = \frac{\delta}{2}\left[\frac{1}{k}\cos(kx_l)+\frac{1}{k+\Delta k}\cos(k+\Delta k)x_l\right], \tag{8}$$

where $x_l=x_0+\xi(x_0,0)$ the initial position of a sheet, is chosen as a new Lagrange coordinate. Now, using Gauss' law $E(x_0,0)=4\pi n_0 e\xi(x_0,0)$ and the initial density profile [Eq. (6)], we get

$$\xi_0(x_0)\sin[\phi_0(x_0)] = -\frac{\delta}{2}\left[\frac{1}{k}\sin(kx_l)+\frac{1}{k+\Delta k}\sin(k+\Delta k)x_l\right]. \tag{9}$$

Squaring and adding Eqs. (8) and (9) and taking the ratio of Eq. (9) to Eq. (8) give $\xi_0(x_0)$ and $\phi_0(x_0)$ in terms of x_l as

$$\xi_0(x_0) = \frac{\delta}{2}\left[\frac{1}{k^2}+\frac{1}{(k+\Delta k)^2}+\frac{2}{k(k+\Delta k)}\cos(\Delta k x_l)\right]^{1/2} \tag{10}$$

and

$$\tan[\phi_0(x_0)] = -\frac{\left[\frac{1}{k}\sin(kx_l)+\frac{1}{k+\Delta k}\sin(k+\Delta k)x_l\right]}{\left[\frac{1}{k}\cos(kx_l)+\frac{1}{k+\Delta k}\cos(k+\Delta k)x_l\right]}. \tag{11}$$

Since $x_l=x_0+\xi(x_0,0)=x_0+\xi_0(x_0)\sin[\phi_0(x_0)]$, Eqs. (10) and (11) represent two coupled transcendental equations for $\xi_0(x_0)$ and $\phi_0(x_0)$. Using the expression for $\xi_0(x_0)$ from Eqs. (10) in (5), the modified plasma frequency finally stands as

$$\tilde{\omega}_{\mathrm{pe}} \approx \omega_{\mathrm{pe}}\left[1-\frac{3}{64}\frac{\omega_{\mathrm{pe}}^2\delta^2}{c^2k^2}\left\{1+\frac{k^2}{(k+\Delta k)^2}+\frac{2k}{(k+\Delta k)}\cos(\Delta k x_l)\right\}\right]. \tag{12}$$

It is clear from the above expression that the nonlinear frequency shift (and hence the modified plasma frequency), for arbitrary value of Δk, is in general space dependent; it depends on the initial position of sheets. This spatial dependence of plasma frequency causes different pieces of the oscillation to go out of phase with time, resulting in a phenomenon called phase mixing. In Fourier space ("k" space), the manifestation of phase mixing is seen by the appearance of higher harmonics (as numerically shown in a later section); the energy which is initially loaded on the modes k and $k+\Delta k$ gradually shifts towards higher "k" values. This gradual transfer of energy from low "k" modes to high "k" modes can be interpreted as damping of the primary wave due to mode coupling to higher modes. The interaction of high "k" modes with particles efficiently takes up energy

from the wave and causes the particles to accelerate and the wave to damp. Further generation of higher harmonics with time also shows up in the particle density profile which becomes more spiky in nature. Eventually phase mixing leads to crossing of electron trajectories which within the cold plasma model results in singularities in the electron density profile (wave breaking). We numerically demonstrate the aforementioned processes in Sec. IV.

The process of phase mixing leading to wave breaking which is characterized by appearance of density spikes, has been observed earlier in nonrelativistic inhomogeneous plasmas where the inhomogeneity is either a static one (infinitely massive ions [11,13,14]) or is self-consistently generated through low-frequency ponderomotive forces which in turn originates from the oscillating electric field of plasma oscillations in the presence of finite mass ion background [15]. As a result of inhomogeneity, plasma frequency becomes a function of position and phase mixing happens. In the present relativistic case, phase mixing occurs even without background inhomogeneity, which as shown above happens due to relativistic variation of electron mass. Hence a relativistically intense wave will always phase mix and eventually break at arbitrarily low values of amplitude δ. Only for the singular case of $\Delta k=0$, does $\tilde{\omega}_{\mathrm{pe}}$ becomes spatially independent and hence does not exhibit phase mixing. For the special case of standing waves, occurrence of wave breaking (appearance of density spikes) has been reported earlier by Infeld *et al.* [16]. In fact for $\Delta k=-2k$, our expression (12) reduces to

$$\tilde{\omega}_{\mathrm{pe}} = \omega_{\mathrm{pe}}\left[1 - \frac{3}{16}\frac{\omega_{\mathrm{pe}}^2\delta^2}{c^2k^2}\sin^2(kx_l)\right] \tag{13}$$

which is Eq. (20) of Ref. [16]. To clearly demonstrate that phase mixing eventually leads to density bursts (wave breaking) and to estimate the phase mixing time scale, we evaluate the electron density in the next subsection.

B. Occurrence of density bursts and phase mixing time

Starting with Gauss' law, we get

$$\frac{\partial E}{\partial x} = 4\pi n_0 e\frac{\partial \xi}{\partial x} = -4\pi e\tilde{n}_e, \tag{14}$$

where $\tilde{n}_e$ is perturbed electron density. Therefore,

$$\frac{\partial \xi}{\partial x_l} = -\frac{\tilde{n}_e}{n_0}\frac{\partial x}{\partial x_l}. \tag{15}$$

Writing $x=x_l-\xi(x_0,0)+\xi(x_0,\tau)$ and substituting for $\partial x/\partial x_l$ in the above equation, the expression for electron density can be written as

$$n_e(x_l,\tau) = \frac{n_0}{1+\dfrac{\partial\xi/\partial x_l}{1-\partial\xi/\partial x_l|_{\tau=0}}}. \tag{16}$$

Computing $\partial\xi/\partial x_l$ using Eqs. (4) and (10)–(12) and substituting in the above expression, we get the final expression for electron density in terms of Lagrange coordinate (x_l,τ) as

$$n_e(x_l,\tau) = \frac{n_0\left[1+\delta\cos\left(\frac{\Delta k}{2}x_l\right)\cos\left(k+\frac{\Delta k}{2}\right)x_l\right]}{1+\delta\cos\left(\frac{\Delta k}{2}x_l\right)\left\{\cos\left(k+\frac{\Delta k}{2}\right)x_l - \cos\left[\left(k+\frac{\Delta k}{2}\right)x_l+\tilde{\omega}_{\mathrm{pe}}\tau\right] + A\omega_{\mathrm{pe}}\tau\sin\left(\frac{\Delta k}{2}x_l\right)\right\}}, \tag{17}$$

where

$$A = \frac{3}{32}\frac{\omega_{\mathrm{pe}}^2\delta^2}{c^2}\frac{\Delta k}{k(k+\Delta k)}\left\{\frac{1}{k}\cos(\tilde{\omega}_{\mathrm{pe}}\tau - kx_l) + \frac{1}{k+\Delta k}\cos[\tilde{\omega}_{\mathrm{pe}}\tau-(k+\Delta k)x_l]\right\}. \tag{18}$$

The secular term which appears in the denominator of Eq. (17) due to the dependence of plasma frequency $\tilde{\omega}_{\mathrm{pe}}$ on the initial position of sheets (x_l), causes the denominator to vanish in a time scale $(\omega_{\mathrm{pe}}\tau_{\mathrm{mix}})$ which is given by

$$\omega_{\mathrm{pe}}\tau_{\mathrm{mix}} \sim \left\{\frac{3}{64}\frac{\omega_{\mathrm{pe}}^2\delta^3}{c^2k^2}\frac{|\Delta k/k|}{|1+\Delta k/k|}\left(1+\frac{1}{|1+\Delta k/k|}\right)\right\}^{-1}. \tag{19}$$

This clearly indicates that phase mixing eventually leads to electron density bursts (wave breaking). For the special case of standing waves $\Delta k=-2k$ (oscillations), Eq. (17) becomes

$$n_e(x_l,\tau) = \frac{n_0[1+\delta\cos(kx_l)]}{1+\delta\cos(kx_l)\left[1-\cos(\tilde{\omega}_{\mathrm{pe}}\tau) - \omega_{\mathrm{pe}}\tau\frac{3}{8}\frac{\omega_{\mathrm{pe}}^2\delta^2}{c^2k^2}\sin^2(kx_l)\sin(\tilde{\omega}_{\mathrm{pe}}\tau)\right]}, \tag{20}$$

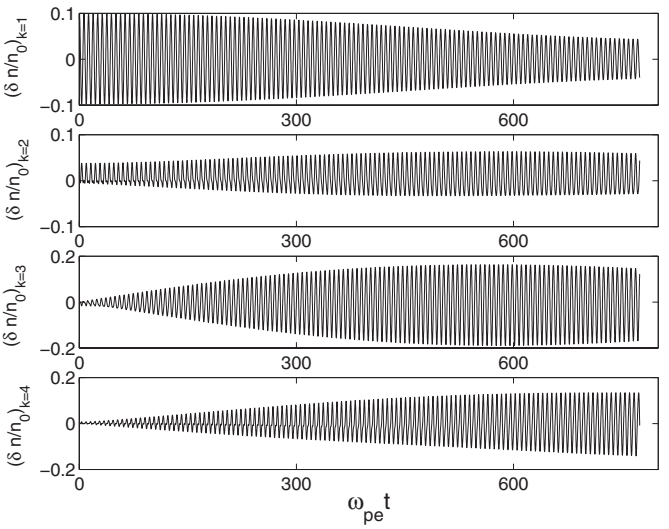

FIG. 1. Temporal evolution of first four density modes for $\delta \sim 0.2$ and $\Delta k/k=-2.0$ (standing waves).

where $\tilde{\omega}_{pe}$ is given by Eq. (13). As expected, Eq. (20) matches Eq. (19) of Ref. [16].

III. NUMERICAL VERIFICATION

Using a code based on Dawson sheet model, we numerically follow the process of phase mixing of two relativistically intense waves separated in wave number by an amount Δk, i.e., we follow the gradual damping of the primary mode (the mode on which energy is initially loaded) along with the simultaneous generation of higher harmonics until it culminates in wave breaking. We also numerically verify the dependence of phase mixing time, Eq. (19), on the amplitude of perturbation δ and the spectral width $\Delta k/k$. For this purpose we have used a one-dimensional sheet code where we have followed the motion of an array of $\sim 10^4$ electron sheets. The

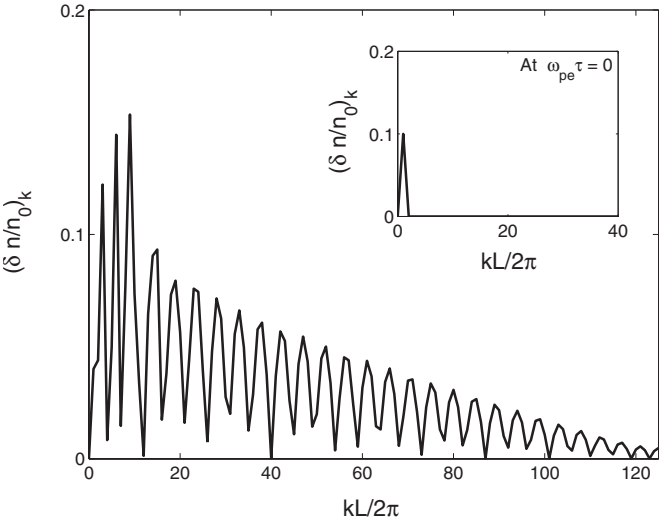

FIG. 2. Number density vs mode number for $\delta \sim 0.2$ and $\Delta k/k=-2.0$ at $\omega_{pe}\tau \sim 0.0$ (inset) and at $\omega_{pe}\tau_{mix} \sim 774.0$ (phase mixing time).

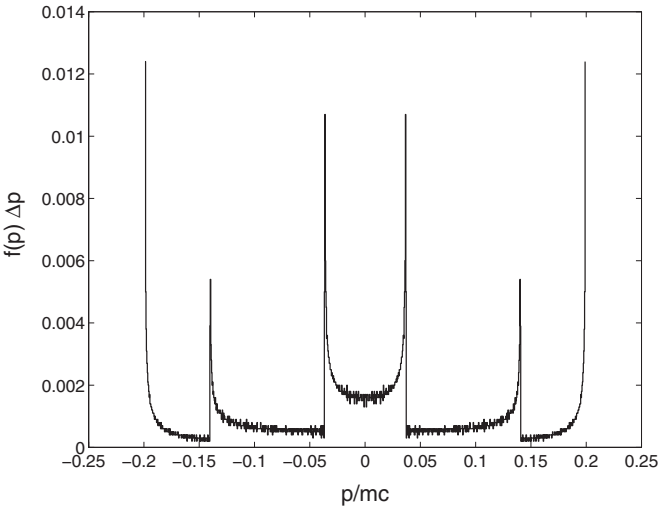

FIG. 3. Momentum distribution for $\delta \sim 0.2$ and $\Delta k/k=-2.0$ at $\omega_{pe}\tau_{mix} \sim 774.0$ (phase mixing time).

sheets are initially loaded in phase space [17] so as to represent the initial density and velocity perturbations as given by Eqs. (6) and (7), respectively. Using these initial conditions, the equation of motion (2) for each sheet is then solved using fourth-order Runge-Kutta scheme. At each time step, ordering of the sheets is checked for sheet crossing. Phase mixing time is measured as the time taken by any two of the adjacent sheets to cross over. We terminate our code at this time, because equation of motion (2) becomes invalid beyond this point. Extension of our code, to take account of sheet crossing will be addressed in future.

Now in order to elucidate the phase mixing process, we have measured the evolution of electron density profile as a function of time. For this purpose we superimpose a spatial grid in the region where the sheets are oscillating, thereby dividing the whole region into cells. The electron density is measured at the cell centres using cloud-in-cell method [17]. Figure 1 shows the time evolution of the first four density

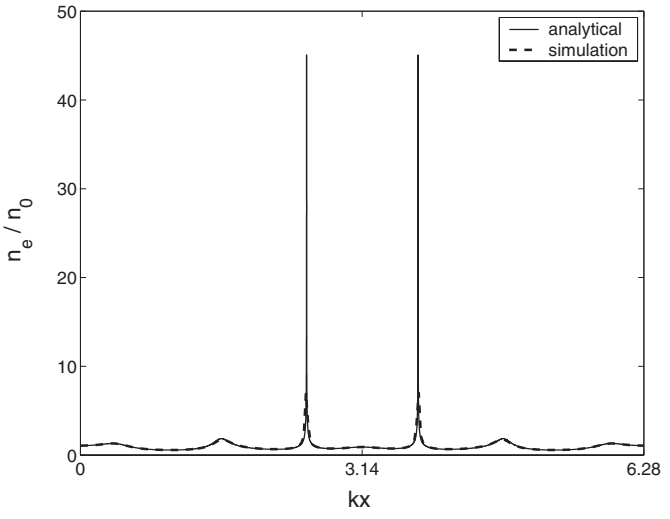

FIG. 4. Density burst near the wave breaking point for $\delta \sim 0.2$ and $\Delta k/k=-2.0$; the broken line shows the numerical profile and the continuous line shows the analytical profile.

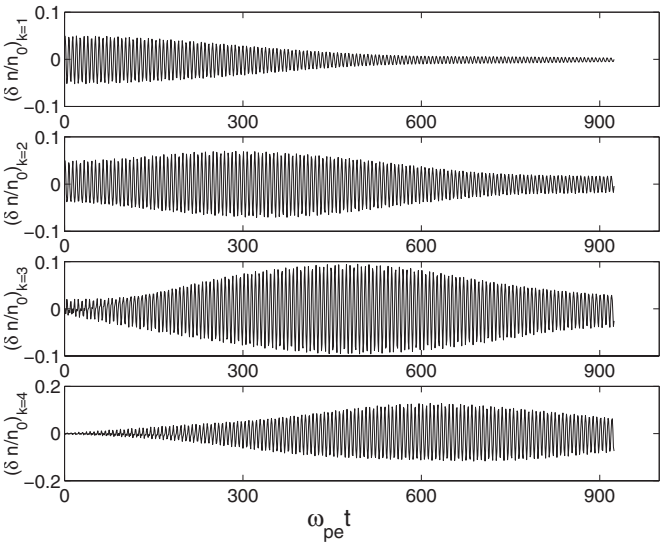

FIG. 5. Temporal evolution of first four density modes for $\delta \sim 0.2$ and $\Delta k/k = -0.5$.

modes for $\delta \sim 0.2$ and $\Delta k/k \sim -2.0$. It clearly shows the decay of the primary mode and the growth of higher harmonics with time. Figure 2 shows the spectrum at $\omega_{pe}\tau = 0$ (see inset) and at $\omega_{pe}\tau_{mix} \sim 774.0$ (phase mixing time). It also shows that the energy which is initially loaded on the primary mode eventually distributes over higher modes. The total energy (kinetic+field) of the system is conserved in our code to order $\sim 10^{-7}$. The interaction of high "k" modes with the particles (sheets) accelerates the particles causing the initial δ-function momentum distribution to spread. Figure 3 shows the momentum distribution at a time close to the phase mixing time ($\omega_{pe}\tau_{mix} \sim 774.0$). It clearly shows generation of multistream flow, another signature of wave breaking [11]. We further show that generation of higher harmonics, in configuration space causes the density profile to become more and more spiky. Figure 4 shows the numerically measured

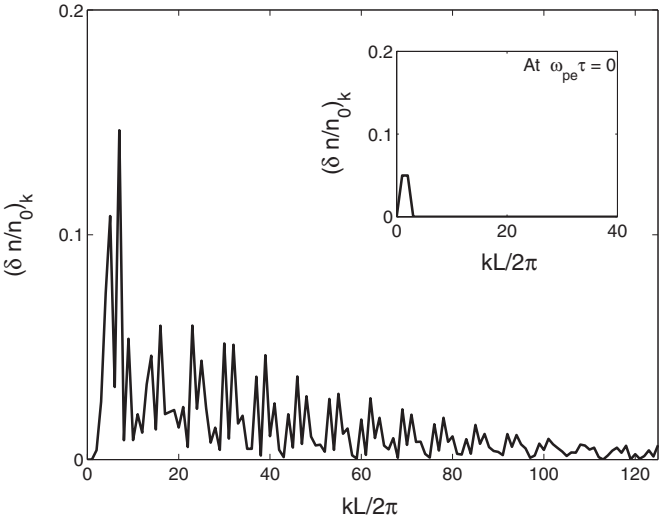

FIG. 6. Number density vs mode number for $\delta \sim 0.2$ and $\Delta k/k = -0.5$ at $\omega_{pe}\tau \sim 0.0$ (inset) and at $\omega_{pe}\tau_{mix} \sim 924.0$ (phase mixing time).

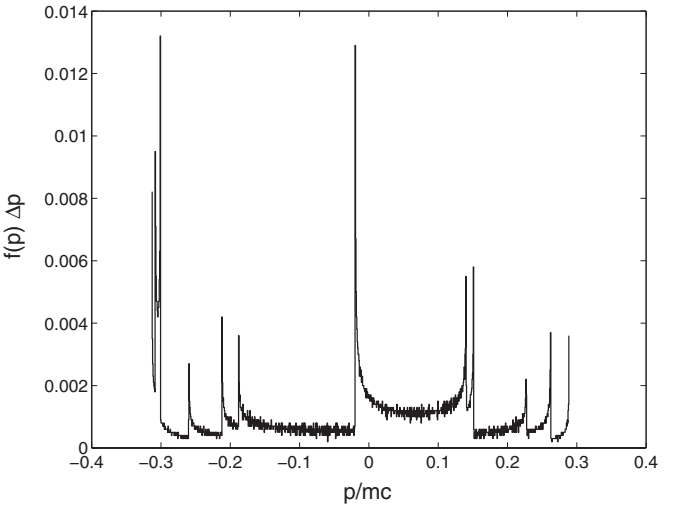

FIG. 7. Momentum distribution for $\delta \sim 0.2$ and $\Delta k/k = -0.5$ at $\omega_{pe}\tau_{mix} \sim 924.0$ (phase mixing time).

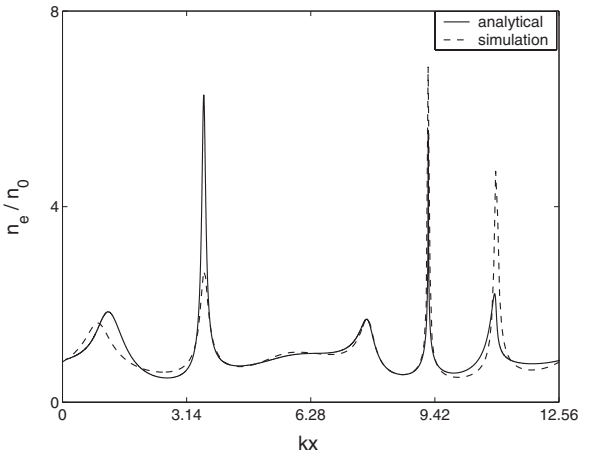

FIG. 8. Density burst near the wave breaking point for $\delta \sim 0.2$ and $\Delta k/k = -0.5$; the broken line shows the numerical profile and the continuous line shows the analytical profile.

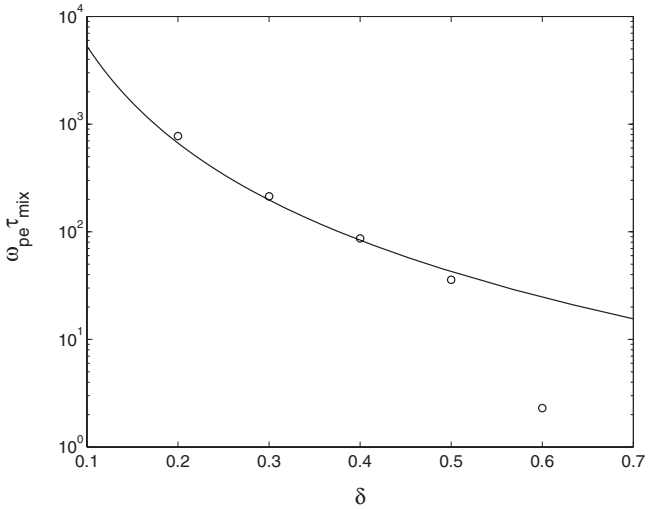

FIG. 9. $\omega_{pe}\tau_{mix}$ vs δ for $\Delta k/k = -2.0$ (standing waves).

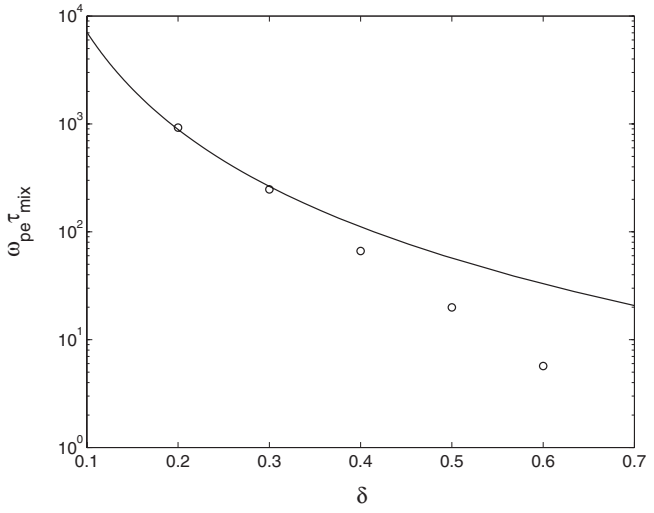

FIG. 10. $\omega_{pe}\tau_{mix}$ vs δ for $\Delta k/k=-0.5$.

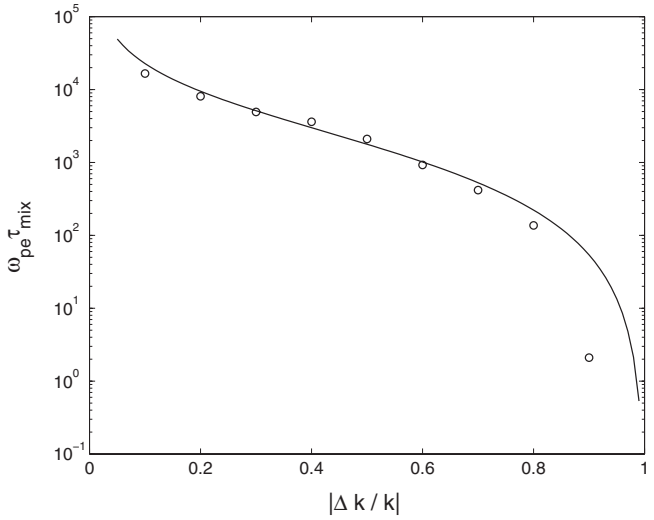

FIG. 11. $\omega_{pe}\tau_{mix}$ vs $|\Delta k/k|$ (for $\delta=0.1$).

density profile along with the analytical expression (17) at a time very close to the phase mixing time. The close fit with numerical results gives good credence to our analytical expressions. Thus (Figs. 1–4 clearly illustrate the processes mentioned in Sec. II A). Figures 5–8 show similar behavior for a different set of parameters $\delta\sim 0.2$ and $\Delta k/k\sim -0.5$.

We now present the variation of phase mixing time with respect to the amplitude of density perturbation and spectral width. Figures 9 and 10 show the variation of phase mixing time with δ for two values of $\Delta k/k$, ~ -2.0 (pure oscillations) and ~ -0.5. The points represent the simulation results and the solid lines represent $\sim 1/\delta^3$ fit. The observed deviation at large δ is due to the breakdown of Bogoliubov approximation around $eE/m\omega_{pe}c\sim 0.6$. Figure 11 shows the variation of phase mixing time with the spectral width $\Delta k/k$ for a fixed value of $\delta\sim 0.1$. Here again, the points represent the simulation results and the solid line represents the fit obtained from Eq. (19). In both cases, the analytical expression (19) shows a very good fit to the observed numerical results, thus vindicating our weakly relativistic calculation.

IV. CONCLUSION

In conclusion, we have shown that a relativistically intense longitudinal wave excited in a cold homogeneous plasma, either by a ultrashort ultraintense laser pulse or by an electron beam pulse will always phase mix and eventually break at arbitrarily low amplitudes and is thus not limited by the Akhiezer-Polovin criterion. Energy when loaded in a low "k" mode, with time gradually gets distributed into high k modes. An important corollary of our work is that, the Akhiezer-Polovin nonlinear longitudinal stationary solution is a solution of zero measure which may decay when subjected to an arbitrarily small amplitude longitudinal perturbation. The decay time (phase mixing time), i.e., the time in which particle orbits cross (wave breaking occurs) is given by $\omega_{pe}\tau_{mix}\sim\{\frac{3}{64}\frac{\omega_{pe}^2\delta^3}{c^2k^2}\frac{|\Delta k/k|}{|1+\Delta k/k|}(1+\frac{1}{|1+\Delta k/k|})\}^{-1}$, where δ is the amplitude of perturbation and $\Delta k/k$ is spectral width of the excited waves. Some early evidence of this damping of wakefield plasma waves can be seen in the experiment of Rosenzweig *et al.* [9]. In that experiment longitudinal plasma waves are excited in the wake of a 21 MeV electron beam pulse propagating through a plasma of density $n_0\sim 2.8\times 10^{13}$ cm^{-3}. From their experimental measurements we can take $\delta\sim 0.48$ and $\Delta k/k\sim -2.0$, giving a phase mixing time of order $\tau_{mix}\sim 160$ ps. Their experimental measurements clearly show damping of the plasma wave of the order of $\sim 44\%$ in 80 ps indicating that in ~ 160 ps the wave should damp completely. For a more precise validation of the mechanism we have proposed in this paper, it would be interesting to carry out experiments that would follow the wave evolution over a longer period. Such experimental verification would facilitate a practical application of our results to plasma based acceleration schemes as well as laser based fusion schemes.

[1] A. I. Akhiezer and R. V. Polovin, Sov. Phys. JETP **3**, 696 (1956).
[2] T. Katsouleas and W. B. Mori, Phys. Rev. Lett. **61**, 90 (1988).
[3] J. B. Rosenzweig, Phys. Rev. A **38**, 3634 (1988).
[4] W. B. Mori and T. Katsouleas, Phys. Scr. **T30**, 127 (1990).
[5] Z. M. Sheng and J. Meyer-ter-Vehn, Phys. Plasmas **4**, 493 (1997).
[6] J. Albritton and G. Rowlands, Nucl. Fusion **15**, 1199 (1975).
[7] C. D. Decker, W. B. Mori, and T. Katsouleas, Phys. Rev. E **50**, R3338 (1994).
[8] L. M. Gorbunov and V. I. Kirsanov, Sov. Phys. JETP **66**, 290 (1987).
[9] J. B. Rosenzweig, P. Schoessow, B. Cole, W. Gai, R. Konecny, J. Norem, and J. Simpson, Phys. Rev. A **39**, 1586 (1989).

[10] V. Saxena *et al.*, Phys. Plasmas **14**, 072307 (2007).
[11] J. M. Dawson, Phys. Rev. **113**, 383 (1959).
[12] N. N. Bogoliubov and V. A. Mitropolsky, *Asymptotic Methods in the Theory of Nonlinear Oscillations* (Hindustan Publishing, Delhi, 1961).
[13] P. K. Kaw *et al.*, Phys. Fluids **16**, 1967 (1973).
[14] E. Infeld, G. Rowlands, and S. Torvén, Phys. Rev. Lett. **62**, 2269 (1989).
[15] S. Sen Gupta and P. K. Kaw, Phys. Rev. Lett. **82**, 1867 (1999).
[16] E. Infeld and G. Rowlands, Phys. Rev. Lett. **62**, 1122 (1989).
[17] C. K. Birdsall and A. B. Langdon, *Plasma Physics via Computer Simulation* (McGraw Hill, New York, 1985).